Met. Mater. Int., Vol. 21, No. 6 (2015), pp. 1091~1100
doi: 10.1007/s12540-015-5276-y

Influence of Punch Face Angle and Reduction on Flow Mode in Backward and Combined Radial Backward Extrusion Process

Jeong-hoon Noh[1], Beong Bok Hwang[1], and Ho Yong Lee[2,*]

[1]Department of Mechanical Engineering, Inha University, 100 Inha-ro, Nam-gu, Incheon 402-751, Korea
[2]Department of Mechanical Engineering, Dongguk University, 30 Pildong-ro 1-gil, Jung-gu, Seoul 100-715, Korea

(received date: 29 May 2015 / accepted date: 13 September 2015)

This paper is concerned with the analysis on the flow mode which determines lubrication limit such as stiction onto or sliding over punch face. The main goal of this study is to examine the influence of geometrical parameters such as punch face angle, reduction in area, and the gap height in radial direction in backward and combined radial-backward extrusion process on the flow mode and surface stresses such as sliding velocity, sliding distance and surface expansion. Annealed steel 17Cr3 was selected as a model material, a rigid-plastic material, for simulation, which was conducted using a commercially available FEA tool, Deform 2-D, programmed in a rigid plasticity theory. Change of flow mode during deformation was also investigated to find under which conditions of process parameter adopted the flow mode changes from stiction to transition or transition to sliding. In this paper, sliding velocities were quantitatively analyzed to determine the flow mode.

Keywords: sliding, friction, metals, extrusion, deformation, interface

1. INTRODUCTION

Two major problems are often encountered in metal forming, particularly in cold extrusion, which is one of the most severe types of metal forming processes. One is the extremely high contact pressure exerted on the workpiece and tool and the pressure might reach over 2500 MPa particularly in the cold extrusion of steels. The other problem is the extreme cold work of certain area on the workpiece surface, which would require the lubricant to stretch 10 to 20 times its original surface area while the lubricant needs to maintain adequate separation of the workpiece and the tool [1-4]. During cold forming experiencing both extremely high contact pressure and surface expansion, a lubricant with the very best separating characteristics is needed for a safe tooling and product [5-7]. The lubricant film thickness as well as surface metal flow is tremendously influenced by the tool geometry and process parameters. Large reductions can be achieved only by adequately controlling surface metal flow while still maintaining the separating lubricant film to prevent metal-to-metal contact under high contact pressure. In metal forming process, a failure of the lubricant film no longer means a simple stretch or gall on the workpiece, but usually means broken tooling and thus shutdowns of entire production line [8].

Danno *et al.* [3] have studied the relationship between localized surface expansion and lubricant film thickness along the inner can wall in case of large reduction and found close correlation between two distributions. Mizno *et al*. [9,10] investigated the influence of reduction and punch nose geometry on the local surface expansion at large reduction. In backward cup extrusion, the influence of punch geometry, strain-hardening, friction factor and reduction was examined experimentally by Bay [11] and numerically by Bennani and Bay [12] on the local surface expansion of the workpiece under the punch. Depending on the process parameters they adopted, three surface flow modes such as sliding, transition or sticking of the workpiece surface was defined at the contact interface of the punch nose and they found correlations between the surface flow mode and the lubrication limit. Recently, Ok *et al*. [1,5] studied numerically the influence of punch face angle, punch corner radius and punch nose diameter on the local surface expansion. Noh *et al*. [13,14] investigated the surface stress profiles in detail at the contact surface in a ring compression test in terms of surface expansion, surface expansion velocity, relative sliding velocity, sliding distance and contact pressure, and found that the surface material flow is significantly dependent of the frictional condition at the tool/workpiece interface. Noh and Hwang [15] also investigated a correlation of surface expansion and forming limit in radial

*Corresponding author: hoyong@dgu.edu

extrusion process, especially the relationship between surface expansion and the formation of surface crack at the flange tip.

In the present study, the backward and combined radial-backward extrusion process were numerically analyzed to examine the influence of punch face angle, reduction in area, and the gap height in radial direction in combined operation on the flow mode and surface stresses distributed on the punch face in terms of sliding velocity, sliding distance, and surface expansion. Annealed steel 17Cr3 was selected as a model material, a rigid-plastic material, for simulation, which was conducted using a commercially available FEA tool, Deform2-D™ [16], programmed in a rigid plasticity theory [17,18]. A solid cylindrical billet was employed for simulation with a diameter of 175.82 mm and a height of 148 mm. The influence of the process parameters such as punch face angle, reduction, and gap height in a combined operation were closely investigated on the surface stresses as well as the surface flow mode, which would help decide if the forming process is safe without lubricant film breakdown and pick-up of the workpiece material on the tool by metal-to-metal contact. The main objective of this study is to reveal the quantitative values which determine the flow mode. The load-stroke relationships were also examined in detail to compare each other between backward and combined radial-backward process. The surface stresses and flow mode characteristics in sequential operations to form a can with flange component were also compared with those in combined operation. The flow mode during backward extrusion process and combined radial backward extrusion process can a determined by distinctive values of surface stresses such as either sliding velocity, sliding distance or surface expansion. The flow mode changes had been predicted such that the topographic contour map of flow mode on punch stroke (h_{st}) and punch face angle (2α) space for different reductions.

2. ANALYSIS AND DISCUSSIONS

In an extrusion process, the die set includes a punch, mandrel and container, of which geometries applied for analysis are shown in Fig. 1. The punch and mandrel geometries recommended by ICFG (International Cold Forging Group) used to be selected for successfully extrusion process to complete the extrusion process successfully [19]. In the figure, the initial and final tool positions are illustrated together with the tool geometries and geometrical process parameters for backward and combined radial/backward processes respectively. A single action process is adopted such that the punch is moving down while the mandrel is stationary during the operation. Due to the nature of symmetry, half of the billet was represented to construct a 2-D axisymmetric model. The punch, mandrel and container were modeled as a rigid body. The punch velocity was kept constant at 1.0 mm/sec. for all simulations. The phosphate-soap was assumed as a lubricant and the friction coefficient at the tool/workpiece interface for simulation was selected as 0.04 [19,20]. The process ended when the punch stroke reached 130 mm and the process parameters are summarized in Table 1. The flow stress is influenced significantly by the strain-rate in a hot forging operation, but in a cold forging the flow stress depends mainly on the strain itself [19]. The material selected for simulation is Annealed steel 17Cr3 [11] of which work-hardening characteristics can be expressed in the form of a power law [21] as shown in the table.

Experiments [11] have revealed that the workpiece material may slide over or stick onto the punch surface during backward extrusion process. Figure 2 shows these two types of flow modes, sliding or stiction. The flow mode, possibly either sliding or stiction, can be determined by observing the flow of workpiece material over the punch surface. In a sliding mode,

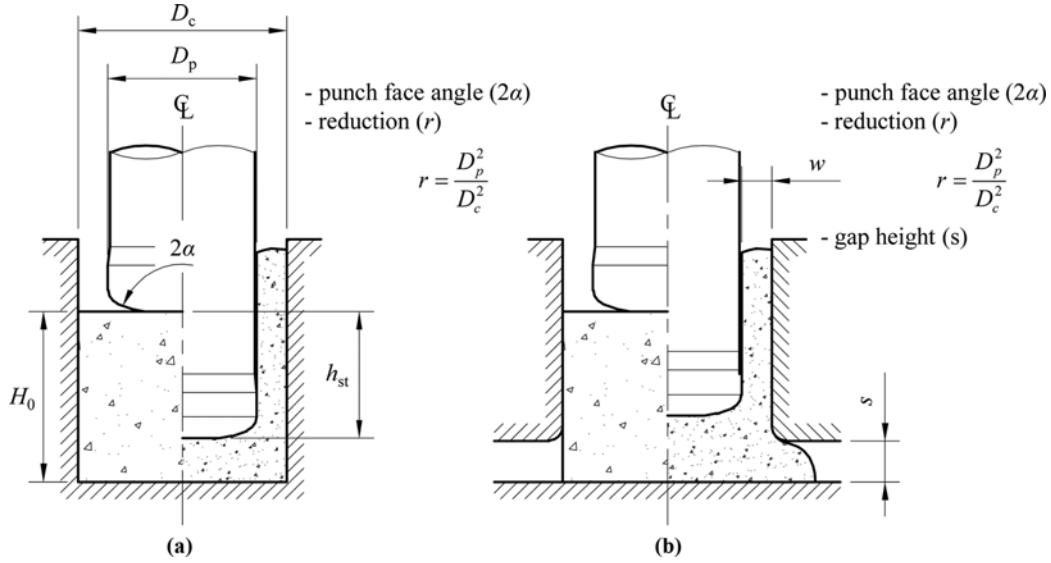

Fig. 1. Schematics of extrusion process. (a) backward extrusion and (b) radial-backward extrusion.

Table 1. Process conditions and parameters used in analysis

Parameter	Values
Initial billet diameter (D_0)	175.8, 101.5 mm
Initial billet height (H_0)	148 mm
Punch diameter (D_p)	55.6 mm
Punch stroke (h_{st})	40 mm
Reduction (r)	0.1, 0.3
Punch face angle (2α)	120°, 135°, 150°, 165°, 180°
Punch face diameter (D_f)	0.6 D_P
Material (Steel 17Cr3)	$\bar{\sigma} = 770\bar{\varepsilon}^{0.17}$
Friction factor (μ)	0.04
Gap width (w)	60.1, 22.9 mm
Gap height (s)	10, 20 mm
Die corner radius (r_c)	3 mm

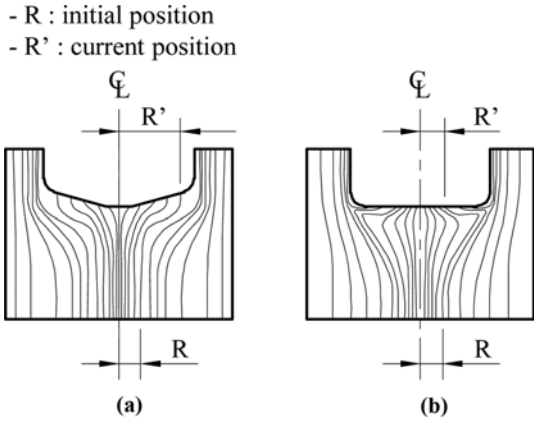

Fig. 2. Flow modes [12]. (a) sliding R'>R and (b) stiction R'≈R.

the workpiece material may slide over the punch surface to some extent, which may cause lubricant film breakdown under the punch nose damaging he workpiece surface. In a full stiction mode, the radial distance from the center axis to the longitudinal lines is almost the same at the workpiece near punch surface as at the bottom of specimen. In a full stiction mode, lubricant can hardly transport to the punch land, which may cause direct metal-to-metal contact between the inner can wall and the punch surface. This is fatal in backward extrusion process. Bennani and Bay [12] performed experiments to reveal the effect of punch face angle on the flow mode for different reductions as shown in Fig. 3. It is easily shown in the figure that the stiction of workpiece material onto the punch surface tends to occur as the punch face angle increases or reduction decreases, respectively.

2.1. Quantitative analysis of flow mode in backward extrusion process

In this section, simulations have been conducted extensively to study the flow mode in quantitative manner based on the experimental results [12]. The surface flow of workpiece is shown in Fig. 4 at different punch strokes for various

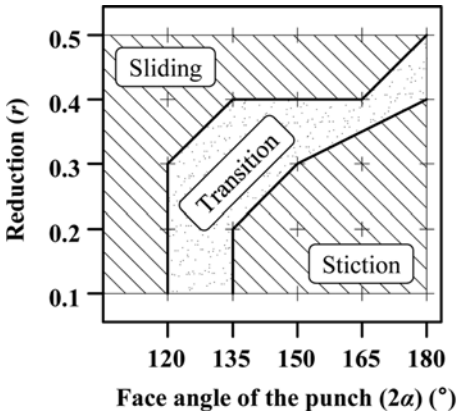

Fig. 3. Topographic contour map of flow mode on reduction (r) and punch face angle (2α) space [12].

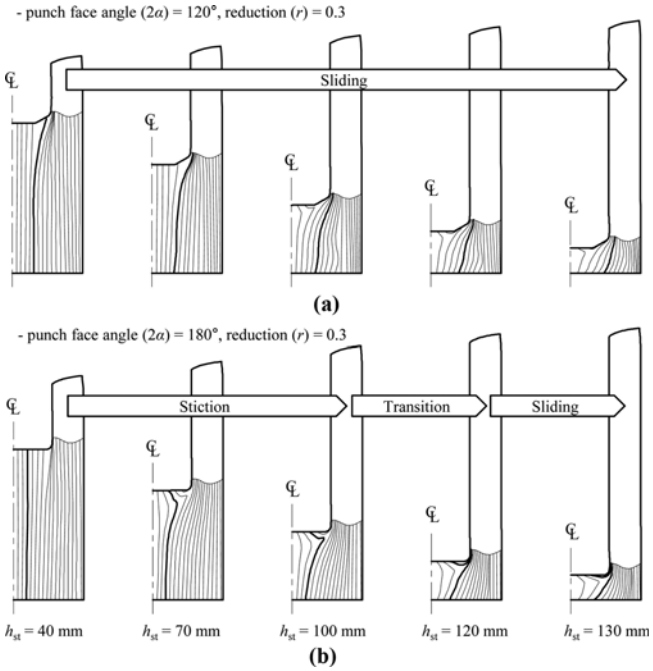

Fig. 4. Flow lines at different punch strokes. (a) punch face angle (2α) = 120°, reduction (r) = 0.3 and (b) punch face angle (2α) = 180°, reduction (r) = 0.3.

punch face angles, under reduction (r) = 0.3. In the figure, initially vertical net in the original billet has been distorted at various stages of deformation process. It is easily known from the figure that the relative motion between workpiece and punch increases as the punch stroke increases and the punch face angle decreases. It was also observed from simulation that the flow mode changes as the deformation process goes on. These calculated flow lines agree qualitatively quite well with the flow mode or flow pattern observed by experiments [12]. More extensive analysis has been performed quantitatively to reveal the flow mode such that the velocity of workpiece in radial direction was calculated as shown in Fig. 5. It is seen in the figure that the radial velocity of work-

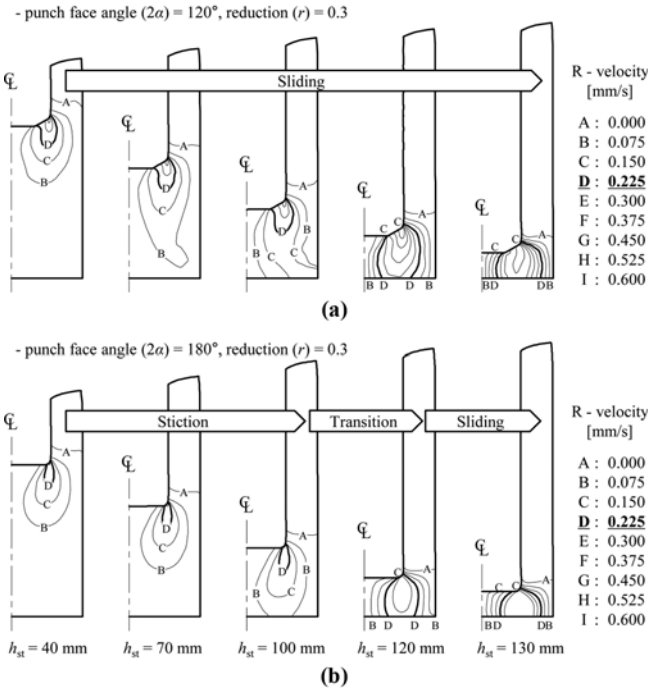

Fig. 5. Velocity distributions in radial direction at different punch face angles. (a) punch face angle (2α) = 120°, reduction (r) = 0.3 and (b) punch face angle (2α) = 180°, reduction (*r*) = 0.3.

piece increases as the punch face angle decreases and increases as the punch stroke increases, leading to relatively large relative motion between punch and workpiece in particular. It is also known in the figure that the relative sliding motion between punch and workpiece is highly localized on the inclined punch surface.

Relative motions of selected cases between punch and workpiece were predicted at different punch strokes for various punch face angles as shown in Fig. 6. It is easily seen in the figure that the sliding velocity increases as the distance increases away from center and this trend is amplified with decrease in punch face angle. It is also observed from the figure that the sliding velocity tends to decrease as the punch face angle increases. In the figure, the sliding velocity tends to increase a little in distance away from center until it reaches the entry of inclined punch surface where it increases abruptly and then again keeps increasing gradually toward the entry of punch corner. It should be noted in the figure that the sliding velocity distribution almost does not change until the punch stroke reaches 110 mm and then overall sliding velocity increases sharply beyond the punch stroke over 110 mm. Change of sliding velocity during deformation process means that the flow mode must change as process proceeds. It can be generally said that sliding speed is not influenced much by the punch stroke under low reduction in height.

Sliding velocity distributions have been predicted at punch stroke of 40 mm for different punch face angles and reductions as shown in Fig. 7. Original sliding velocity distribution was normalized to non-dimensional value by punch speed, punch diameter and the radial distance from center. The predictions were achieved for punch stroke of 40 mm to compare the simulation results to those from experiments [12], and then to determine the flow mode in quantitative manner. It is seen again in the figure that the sliding velocity tends to increase as the distance from center increases. This trend is intensified with decreasing punch face angle and increasing reduction. The dashed lines were drawn based on the experiments and characterize the relative motion between punch and workpiece as stiction mode under the normalized sliding velocity of 0.55 and as sliding mode over 0.65. The transition mode is defined as the normalized sliding velocity between 0.55 and 0.65.

2.2. Effect of punch face angle and reduction on sliding distance and surface expansion

Sliding distance distributions have been calculated at punch stroke of 40 mm for different punch face angles and reduc-

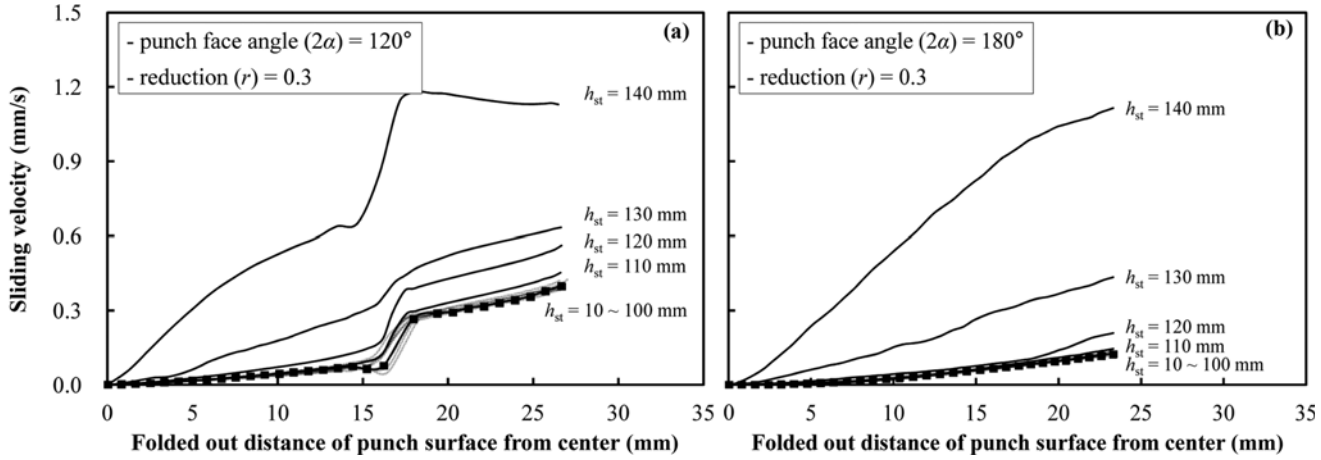

Fig. 6. Sliding velocity (V_S) distributions at different punch strokes for various punch face angles. (a) punch face angle (2α) = 120°, reduction (r) = 0.3 and (b) punch face angle (2α) = 180°, reduction (*r*) = 0.3.

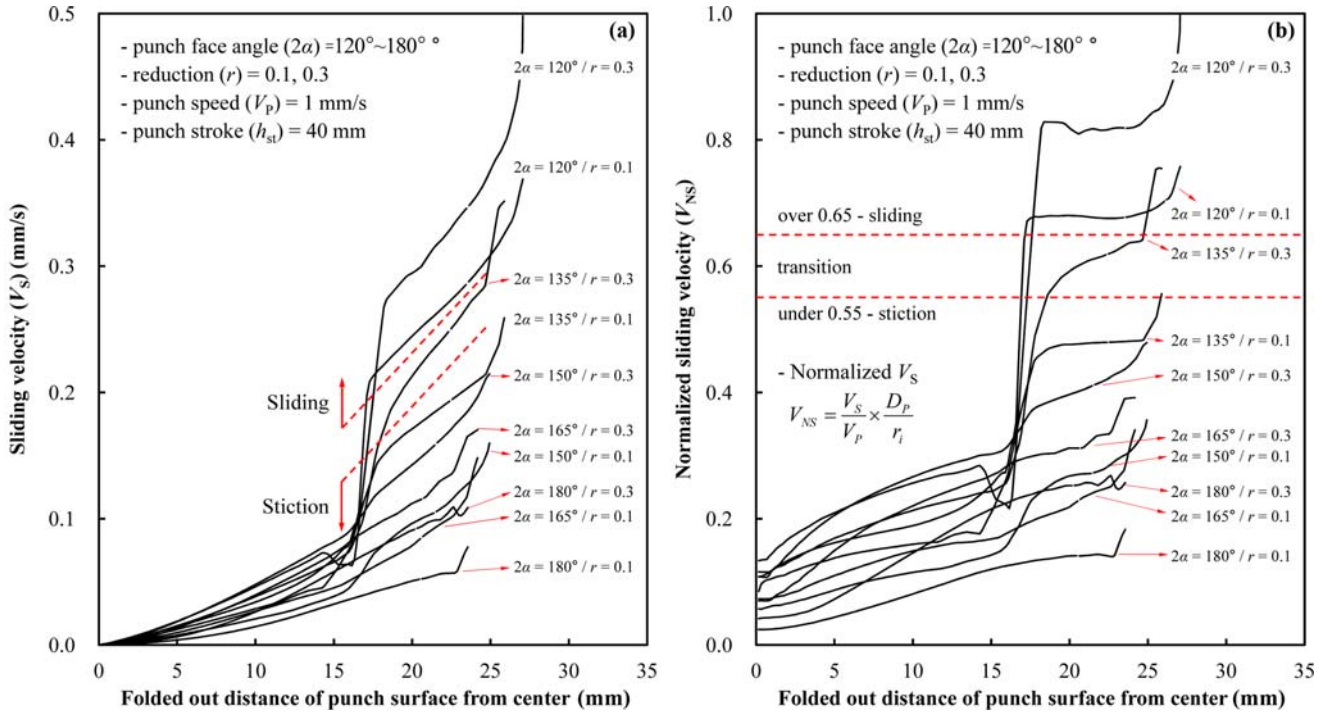

Fig. 7. Original (V_S; left) and normalized sliding velocity (V_{NS}; right) distributions for various punch face angles (2α) and reductions (r). (a) original sliding velocity and (b) normalized sliding velocity.

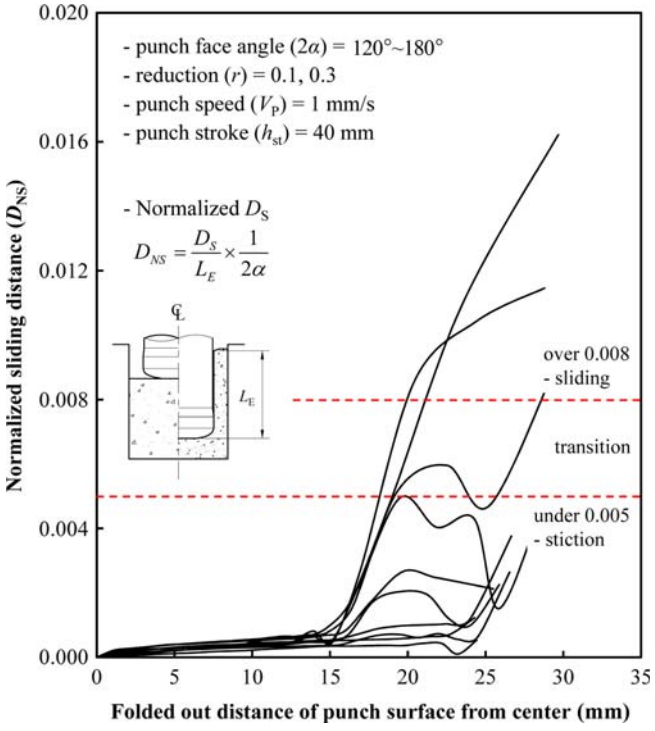

Fig. 8. Normalized sliding distance (D_{NS}) distributions for various. punch face angle (2α) and reduction (r).

tions as shown in Fig. 8, which represents the effect of punch face angle (2α) and reduction (r) on sliding distance of workpiece on the particular location of moving punch surface. It should be noted that the sliding distance was normalized to non-dimensional value by backward can height and punch face angle. Sliding distance together with sliding speed contact pressure is an important surface stress and can be used to predict tool life and/or failure in terms of wear. It is clearly seen in the figure that sliding distance tends to increase a little as the distance increases away from center until it reaches in regions near the entry of punch corner or the entry of inclined punch surface, where sliding distance rises sharply and shows highly localized value. The localization of sliding distance increases as punch face angle decreases and this trend is amplified with increase in reduction. As seen in the figure, the normalized sliding distance can be also used to determine the flow mode such that the value of normalized sliding distance is less than 0.005 for full stiction and greater than 0.008 for sliding mode. In transition mode, it is clear from the figure that the value of normalized sliding distance is between 0.005 and 0.008.

Large surface expansion together with stiction of workpiece to the punch face may lead to lubricant film breakdown, pick-up, and cold welding to the land during cold forging process, and has to be avoided. The effect of punch face angle (2α) and reduction (r) on surface expansion has been predicted at the punch stroke of 40 mm and is shown in Fig. 9. It should be noted again that the surface expansion was normalized to non-dimensional value by backward can height, punch face angle, and punch diameter. It is clearly known from the figure that the localized value of surface expansion

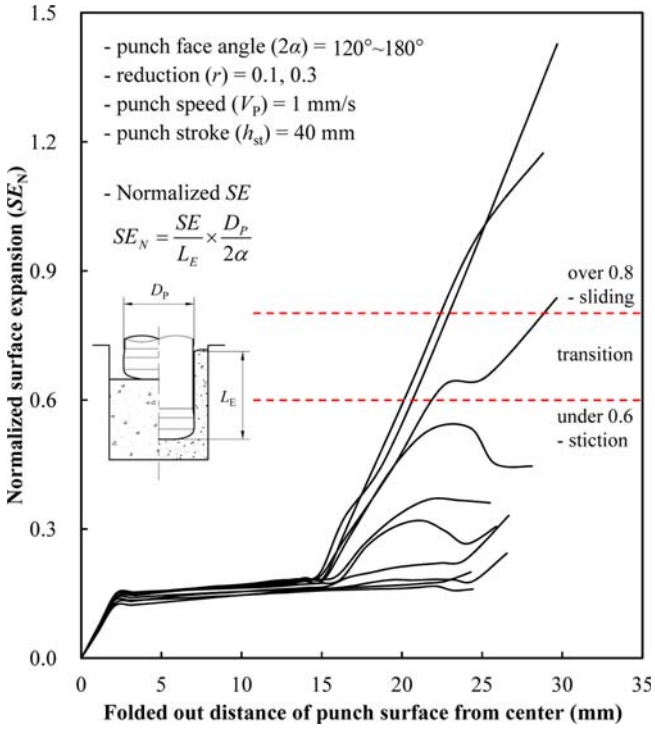

Fig. 9. Normalized surface expansion (SE_N) distributions for various punch face angle (2α) and reduction (r).

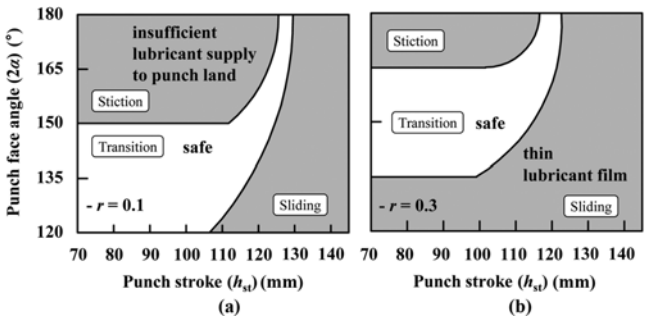

Fig. 10. Topographic contour map of flow mode on punch stroke (hst) and punch face angle (2α) space for different reductions (r). (a) reduction (r) = 0.1 and (b) reduction (r) = 0.3.

increases as punch face angle decreases and the tendency is intensified with increase in reduction. It is easily seen in the figure that the normalized surface expansion generally increases as the distance increases away from center. However, the normalized surface expansion tends to keep more or less constant until it reaches in regions near the entry of punch corner or the entry of inclined punch surface, where surface expansion rises sharply and shows highly localized value. It is generally known that the distribution pattern of surface expansion seems very similar to those of sliding distance. So far in this study, it was revealed that flow mode during backward extrusion process can be determined by distinctive values of surface stresses such as either sliding velocity, sliding distance or surface expansion, which is summarized in Table 2.

It is interesting to see the flow mode changes during backward extrusion process. Figure 10 shows the topographic contour map of flow mode on punch stroke (h_{st}) and punch face angle (2α) space for different reductions. It is clearly seen in the figure that full stiction mode tends to occur as the punch face angle increases and the tendency is increasing with decrease in reduction. It is also known generally from the figure that sliding mode is likely to happen as the punch stroke increases, i.e. deformation proceeds. The transition zone tends to become narrow as the punch stroke increases. It can be generally recommended from the figure that punch face angle between 120° and 150°, and between 135° and 165° would be safe for successful backward extrusion in terms of tribology for the punch stroke less than about 100 mm. It can be also concluded from the figure that punch face angle is a dominant parameter affecting the flow modes while the reduction is not a significant process parameter influencing on the surface flow mode.

2.3. Prediction of flow mode in combined radial-backward extrusion process

Several processes or operations can be executed by one stroke in a single tool in a combined process. In metal forming, it is not usually possible to form a cold-formed component in a single operation. To obtain more complex geometries and net shape or near net shape qualities, process combinations or process sequences are employed. The combined operations have the advantages of saving operations and tools, probably omitting possible intermediate treatments, and giving a combined process economical lead [22]. Simultaneous completion of material flow in the two directions is almost impossible in combined operations because of the cavity extrusion ratios and lengths in forward and radial directions. Therefore, control of material flow is extremely important for reducing the

Table 2. Surface stresses characterizing flow modes

		Stiction	Transition	Sliding
Normalized sliding velocity (V_{NS})	$V_{NS} = \frac{V_S}{V_P} \times \frac{D_P}{r_i}$	under 0.55	0.55 ~ 0.65	Over 0.65
Normalized sliding distance (D_{NS})	$D_{NS} = \frac{D_S}{L_E} \times \frac{1}{2\alpha}$	under 0.005	0.005 ~ 0.008	over 0.008
Normalized surface expansion (SE_N)	$SE_N = \frac{SE}{L_E} \times \frac{D_P}{2\alpha}$	under 0.6	0.6 ~ 0.8	over 0.8

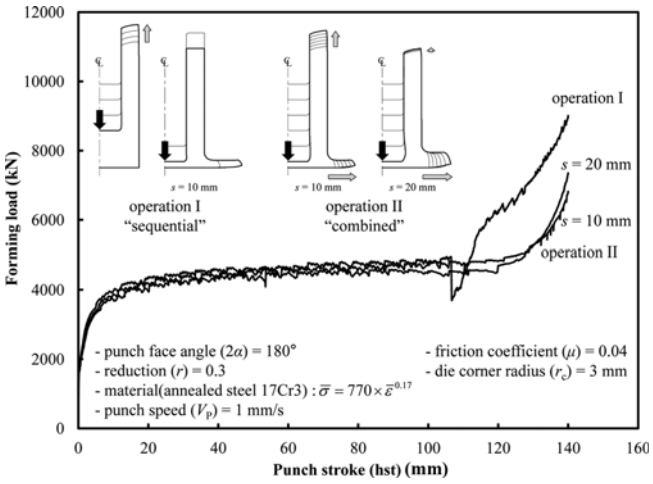

Fig. 11. Load-stroke relationships for sequential and combined operations.

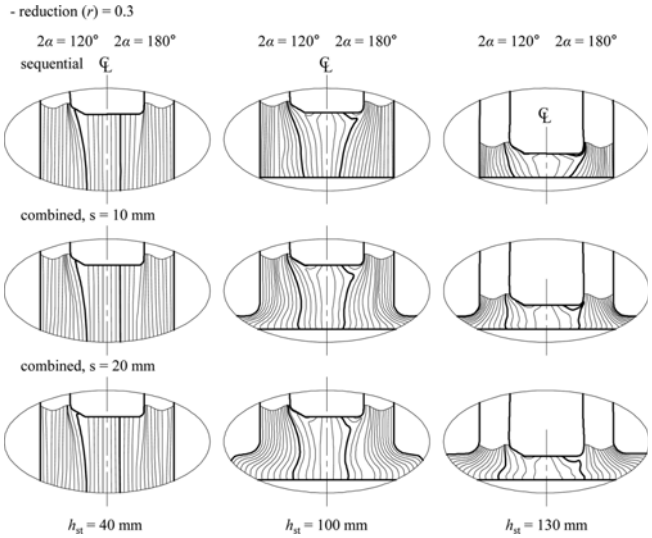

Fig. 12. Comparison of flow lines of backward and combined processes at different punch strokes.

extrusion pressure at the final stage of the operation in order to take advantage of the combined process [23,24].

In this section, the influence of tool geometry such as punch face angle, reduction, and gap height between upper and lower die has been investigated in terms of comparison of forming load between sequential and combined operation, material flow characteristics, surface stresses on the punch surface, and flow mode analysis in combined radial-backward extrusion process. Furthermore, the flow mode in backward extrusion process, which is explained in previous section, is compared to those in combined operation.

Radial-backward extrusion processes were simulated both for a combined operation in one stroke and for sequential operations with multi forming stations. Figure 11 represents the load-stroke relationships for different process sequences. In sequential operations, the billet was extruded in the radial direction after extruded in the backward direction, while in a combined operation the billet was pressed by a punch, allowing the material flow into both directions simultaneously. The simulation was performed by adopting the process parameters such that the value of punch face angle was selected as 180°, the reduction as 0.3, and the radial gap height as both 10 and 20 mm for combined operation. It can be easily known from the figure that the maximum force requirement is pretty high in a sequential operation comparing to that in a combined operation. As seen in the figure, the forming load in a backward extrusion in sequential operation is very similar to those in a combined operation, i.e. until the punch stroke reaches about 100 mm. However, the forming load rises sharply during radial extrusion process in a sequential operation and the maximum punch load reaches about 9000 kN at the end of sequential operations, i.e. at the completion of radial extrusion process, which is pretty higher than those in combined operations. It is naturally revealed from the figure that the forming load is not influenced much by the radial gap height in combined operations.

The surface flow of workpiece in backward and combined operations were calculated at different punch strokes, i.e. h_{st} = 40, 100, 130 mm, for various punch face angles, i.e. $2\alpha = 120°$ and 180° and different gap heights (s) in combined operation such as s = 10 and 20 mm, and is shown in Fig. 12. It should be noted that the reduction applied for simulation is 0.3. The initial vertical net in the original billet has been distorted at various stages of deformation as the process proceeds. It is easily seen again from the figure that the relative motion between workpiece and punch increases as the punch stroke increases enough, i.e. beyond 100 mm, and the punch face angle decreases regardless of the operation type, backward or combined, and of gap height. It was also observed from simulation that the flow mode changes as the deformation process goes on. In the figure, more relative motion between punch and workpiece is observed in combined operation than in backward operation in this particular case, i.e. $r = 0.3$.

Surface stresses such as normalized sliding velocity, sliding distance, and surface expansion distributions on the particular location of moving punch surface were predicted in combined operations and they are shown in Fig. 13. It should be noted that the predictions were performed at the punch stroke of 40 mm for all cases of simulations. It can be generally seen in the figure that the normalized sliding velocity increases as the distance increases away from center and the tendency is intensified with decrease in punch face angle and increase in reduction. It is also observed in the figure that the relative motion between punch and workpiece, i.e. sliding velocity, generally decreases as the gap height increases. For the punch face angle of 180°, i.e. flat punch, the relative motion increases gradually as the distance increases away from center regardless of reduction and gap height. However, the rel-

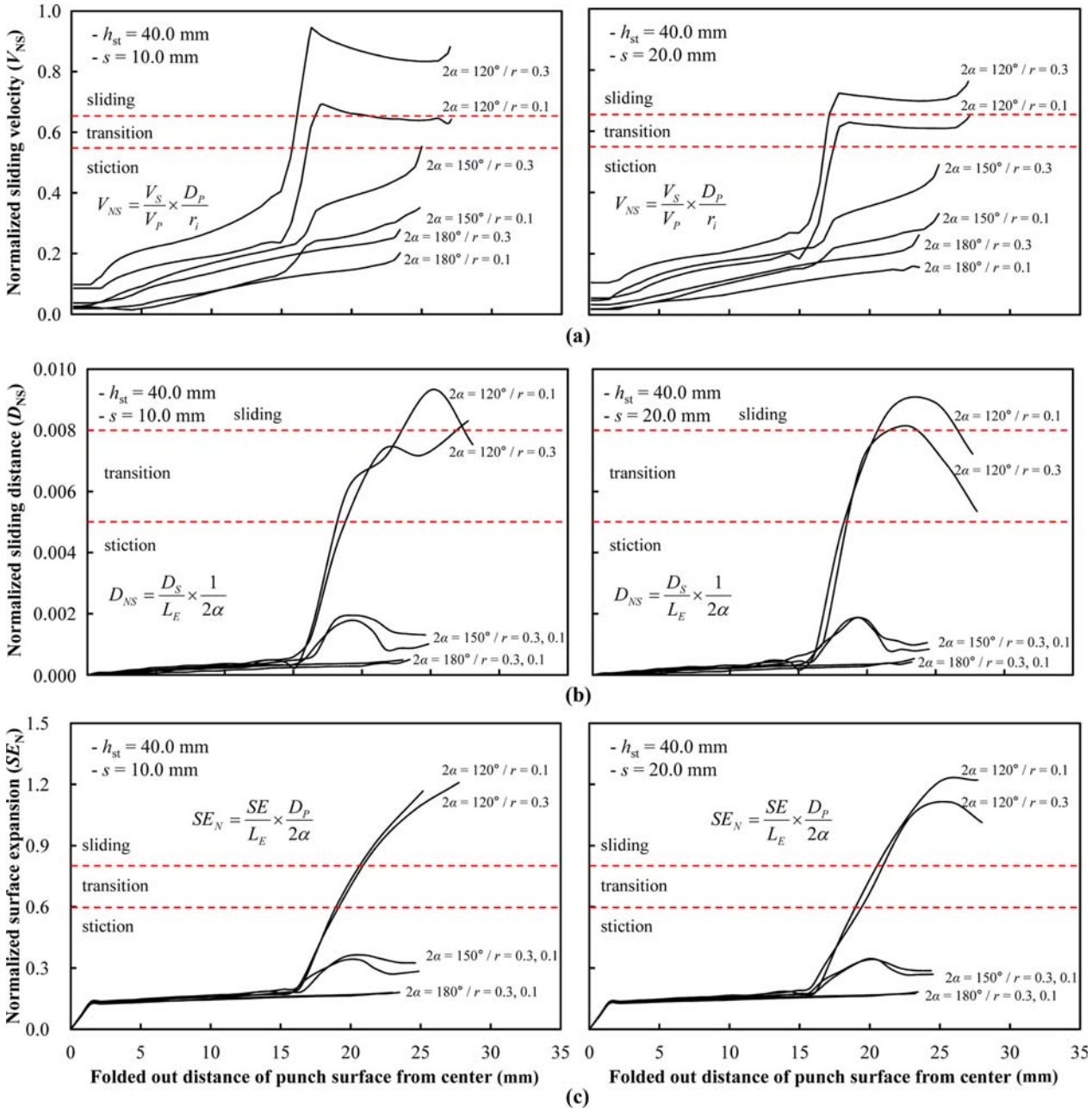

Fig. 13. Normalized sliding velocity, sliding distance and surface expansion distributions. (a) normalized sliding velocity, (b) normalized sliding distance, and (c) normalized surface expansion.

ative motion rises sharply in regions near the entry of inclined punch surface and this trend is amplified with decrease in punch face angle.

The normalized sliding distance distributions on the particular location of moving punch surface are also seen in the figure. For flat punch, i.e. $2\alpha = 180°$, the sliding distance increases a little as the distance increases away from center. However, the sliding distance increases sharply in regions near the entry of inclined punch surface and the tendency is intensified with decrease in punch face angle and reduction. It is observed in the figure that the difference of sliding distance distributions for different gap heights seems insignificant. The normalized surface expansion distributions were also predicted as seen in the figure. It is generally known from the figure that the surface expansion distributions are pretty much similar to those of sliding distance.

Figure 14 shows the topographic contour map of flow mode on punch stroke (h_{st}) and punch face angle (2α) space for different reductions and gap heights. It is clearly seen again in the figure that full stiction mode tends to occur as the punch

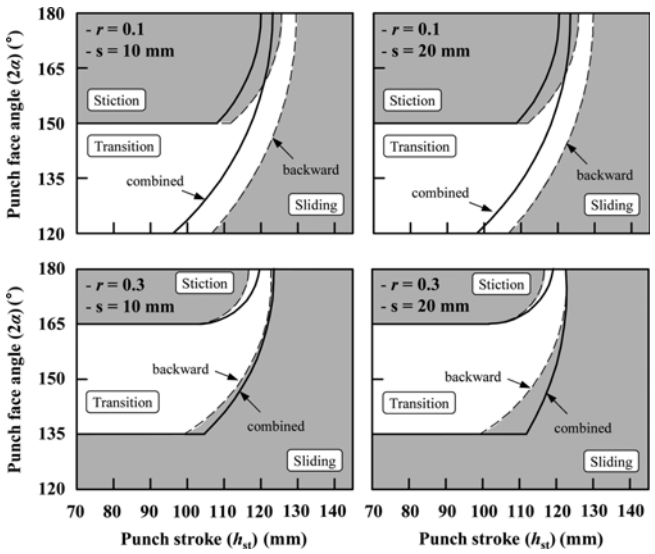

Fig. 14. Relationship between punch stroke and punch face angles (2α) for different reductions (*r*) and gap heights (*s*).

face angle increases and the tendency is increasing with decrease in reduction. It is also known generally from the figure that sliding mode is likely to happen as the punch stroke increases, i.e. deformation proceeds. The transition zone tends to become narrow as the punch stroke increases. Comparing to those in backward operation (dashed line), it can be said from the figure that in combined operation the transition zone, i.e. relatively safe in view of tribological condition, becomes large in terms of reduction in height for low reduction, i.e. $r = 0.3$, regardless of gap height. However, the story is opposite for large reduction, i.e. $r = 0.1$, such that the transition zone is relatively small comparing to those for backward extrusion process. In combined operation, it can be generally recommended from the figure that punch face angle between 120° and 150° would be safe for reduction $r = 0.1$, and between 135° and 165° for reduction $r = 0.3$ for successful combined operation in terms of lubrication limit until the punch stroke reaches about 95 mm for reduction $r = 0.1$ and about 110 mm for reduction $r = 0.3$, respectively. It is also observed again from the figure that punch face angle is a dominant parameter affecting the flow modes while the reduction and gap height in combined operation are not a significant process parameter influencing on the surface flow mode.

Figure 15 shows the topographic contour map of stiction and sliding zone on punch face angle (2α) and reduction (*r*) space for sequential (dashed line) and combined (solid line), and for gap height s = 10 mm and 20 mm. It is easily seen in the figure that the transition zone in combined operation is larger than those in sequential operation for large reduction, i.e. $r = 0.3$. This trend is amplified with increase in gap height. However, the transition zone in combined operation seems smaller than those in sequential operation for small reduction, i.e. $r = 0.1$, and the tendency is intensified with increase in gap height. It can be generally concluded from the figure that a combined operation is safer than a sequential operation for large reduction purely in terms of a tribological condition such as lubrication limit. It is proven again from the figure that severe tribological conditions are more likely to occur at low reduction regardless of operation type, sequential or combined.

3. CONCLUSIONS

In the present study, backward and combined radial-backward extrusion process were numerically analyzed to investigate the influence of punch face angle, reduction, and gap height in radial direction on the surface stresses along contact boundary and the flow modes affecting lubricant transport. The present study was focused to reveal the quantitative value of sliding velocity determining the flow mode and surface stress characteristics in backward and combined radial-backward extrusion processes. In this paper, as an original

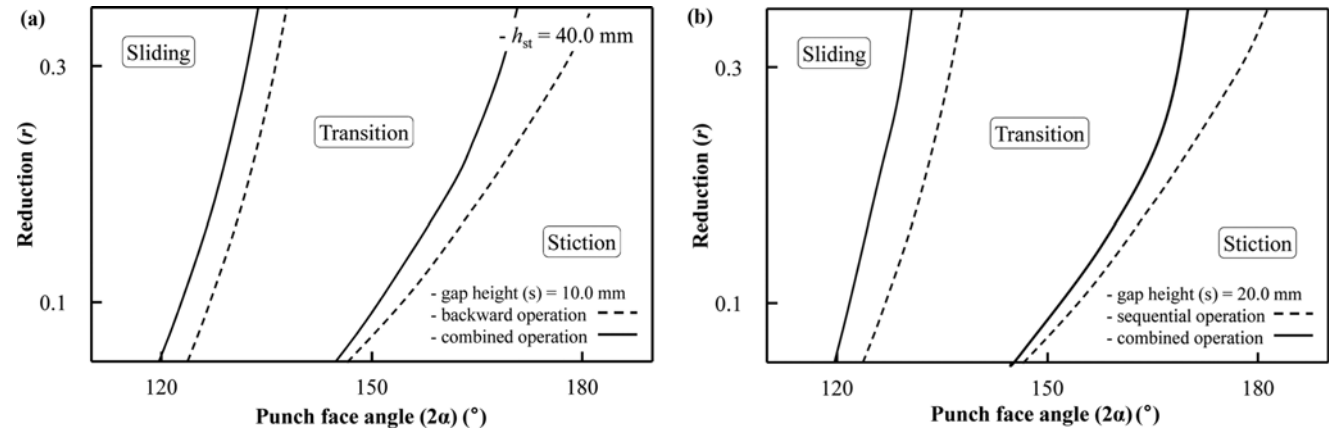

Fig. 15. Flow modes in backward and combined operation on punch face angle (2α) and reduction (*r*) space. (a) gap height (s) = 10.0 mm and (b) gap height (s) = 20.0 mm.

finding, the flow mode changes had been predicted during the process for different process parameters such that the topographic contour map of flow mode on punch stroke (h_{st}) and punch face angle (2α) space for different reductions. The Characteristics of flow mode for different process parameters and process sequences are summarized as follows;

(1) In backward operation, the sliding velocity tends to decrease as the punch face angle increases and is not influenced much by the punch stroke under low reduction in height. The distinctive values of normalized sliding velocities were found such that the flow mode is stiction in range of velocity between 0 and 0.55, transition between 0.55 and 0.65, and sliding over 0.65, respectively. The flow mode during backward extrusion process can be determined by distinctive values of surface stresses such as either sliding velocity, sliding distance or surface expansion.

(2) Full stiction mode tends to occur as the punch face angle increases and the tendency is increasing with decrease in reduction. Sliding mode is likely to happen as the punch stroke increases, i.e. deformation proceeds. The transition zone tends to become narrow as the punch stroke increases. It is generally recommended that punch face angle between 120° and 150°, and between 135° and 165° would be safe for successful backward extrusion in terms of tribology for the punch stroke less than about 100 mm. The punch face angle was found to be a dominant parameter affecting the flow modes while the reduction is not a significant process parameter influencing on the surface flow mode.

(3) In combined operation, full stiction mode tends to occur as the punch face angle increases and the tendency is increasing with decrease in reduction. The sliding mode is likely to happen as the punch stroke increases, i.e. deformation proceeds. Comparing to backward operation, the transition zone, i.e. relatively safe in view of tribological condition, becomes large in terms of reduction in height for low reduction, i.e. $r = 0.1$, regardless of gap height. However, for large reduction, i.e. $r = 0.3$, the transition zone is relatively small comparing to those for backward extrusion process.

ACKNOWLEDGMENT

This research was supported by Inha & Dongguk University Research Grant in 2015.

REFERENCES

1. J. H. Ok and B. B. Hwang, *Mater. Sci. Forum* **519-521**, 931 (2006).
2. K. H. Min, J. M. Seo, H. S. Koo, V. R. Jayasekara, S. H. Tak, I. C. Lee, and B. B. Hwang, *Trans. Mater. Process*. **16**, 521 (2007).
3. A. Danno, K. Abe, and F. Nonoyama, *J. Jap. Soc. Technol. Plastic*. **24**, 213 (1983).
4. H. Y. Lee, J. H. Noh, and B. B. Hwang, *Tribol. Int*. **64**, 215 (2013).
5. K. H. Min, V. R. Jayasekara, B. B. Hwang, and D. H. Jang, *Trans. Mater. Process*. **16**, 582 (2007).
6. S. H. Park, H. S. Kim, and B. S. You, *Korean J. Met. Mater*. 51, 637 (2013).
7. S. H. Park, H. S. Kim, and B. S. You, *Met. Mater. Int*. **20**, 291 (2014).
8. American Society for Metals, *Source Book on Cold Forming*, p.16, The Periodical Publication Department American Society for Metals, Ohio, USA (1975).
9. T. Mizuno, Y. Kojima, K. Kitamura, and W. Zhu, *J. Jap. Soc. Technol. Plastic*. **25**, 929 (1984).
10. T. Mizuno, W. Zhu, Y. Kojima, and K. Sugimoto, *J. Jap. Soc. Technol. Plastic*. **28**, 1060 (1987).
11. N. Bay, S. Lassen, K. B. Pedersen, and V. Maegaard, *Ann. CIRP.* **40**, 239 (1991).
12. B. Bennani and N. Bay, *J. Mater. Process. Technol*. **61**, 275 (1996).
13. J. H. Noh, M. T. Kim, and B. B. Hwang, *J. Mech. Sci. Technol*. **24**, 1611 (2010).
14. J. H. Noh, K. H. Min, and B. B. Hwang, *Tribol. Int.* **44**, 947 (2011).
15. J. H. Noh and B. B. Hwang, *Steel Res. Int.* **81**, 450 (2010).
16. Scientific Forming Technologies Corporation, *Deform 2-D TM User Manuals*, pp.4-17, Scientific Forming Technologies Corporations Inc., Ohio, USA (2004).
17. C. H. Lee and S. Kobayashi, *J. Manuf. Sci. Eng*. **95**, 865 (1973).
18. Y. P. Song, W. K. Wang, D. S. Gao, E. Y. Yoon, D. J. Lee, and H. S. Kim, *Met. Mater. Int*. **20**, 445 (2014).
19. J. H. Noh and B. B. Hwang, *Met. Mater. Int.* **19**, 1193 (2013).
20. G. Ngaile, H. Saiki, L. Ruan and Y. Marumo, *Wear* **262**, 684 (2007).
21. B. B. Hwang, J. H. Shim, J. M. Seo, H. S. Koo, J. H. Ok, Y. H. Lee, G. M. Lee, K. H. Min, and H. J. Choi, *Mater. Sci. Forum* **519-521**, 949 (2006).
22. W. Osen, *Proc. Adv. Technol. Plastic. Conf.* (eds. K. Lange), p.575, Springer, Stuttgart, West Germany (1987).
23. D. H. Jang, J. H. Ok, G. M. Lee, and B. B. Hwang, *Mater. Sci. Forum* **519-521**, 955 (2006).
24. B. D. Ko, H. J. Choi, D. H. Jang, J. Y. Lim, and B. B. Hwang, *Trans. Mater. Process.* **12**, 251 (2003).